

PCCP

Accepted Manuscript



This is an *Accepted Manuscript*, which has been through the Royal Society of Chemistry peer review process and has been accepted for publication.

Accepted Manuscripts are published online shortly after acceptance, before technical editing, formatting and proof reading. Using this free service, authors can make their results available to the community, in citable form, before we publish the edited article. We will replace this *Accepted Manuscript* with the edited and formatted *Advance Article* as soon as it is available.

You can find more information about *Accepted Manuscripts* in the [Information for Authors](#).

Please note that technical editing may introduce minor changes to the text and/or graphics, which may alter content. The journal's standard [Terms & Conditions](#) and the [Ethical guidelines](#) still apply. In no event shall the Royal Society of Chemistry be held responsible for any errors or omissions in this *Accepted Manuscript* or any consequences arising from the use of any information it contains.

Where does methanol lose hydrogen to trigger steam reforming? A revisit of methanol dehydrogenation on the PdZn alloy model obtained from kinetic Monte Carlo simulations

Feng Cheng, Zhao-Xu Chen*

Institute of Theoretical and Computational Chemistry, Key Laboratory of Mesoscopic Chemistry of MOE, School of Chemistry and Chemical Engineering, Nanjing University, Nanjing, 210093, P.R. China

Abstract: Pd/ZnO is a promising catalyst studied for methanol steam reforming (MSR) and 1:1 PdZn alloy is demonstrated to be the active component. It is believed that MSR starts from methanol dehydrogenation to methoxy. Previous studies of methanol dehydrogenation on the ideal PdZn(111) surface shows that methanol adsorbs weakly on the PdZn(111) surface and it is hard for methanol to transform into methoxy because of the high dehydrogenation barrier, indicating that the catalyst model is not appropriate for investigating the first step of MSR. Using the model derived from our recent kinetic Monte Carlo simulations, we examined the process $\text{CH}_3\text{OH} \rightarrow \text{CH}_3\text{O} \rightarrow \text{CH}_2\text{O} \rightarrow \text{CHO} \rightarrow \text{CO}$. Compared with the ideal model, methanol adsorbs much more strongly and the barrier from $\text{CH}_3\text{OH} \rightarrow \text{CH}_3\text{O}$ is much lower than on the kMC model. On the other hand, the C-H bond breaking of CH_3O , CH_2O and CHO becomes harder. We show that co-adsorbed water is important for refreshing the active sites. The present study shows that the first MSR step most likely takes place on three-fold hollow sites formed by Zn atoms, and the inhomogeneity of PdZn alloy may exhibit significant influence on reactions.

* Corresponding author. Fax: +86 2583593353. E-mail address: zxchen@nju.edu.cn

1 Introduction

Methanol is an ideal energy carrier used to produce clean energy source, hydrogen. Methanol dehydrogenation ($\text{CH}_3\text{OH} = \text{CO} + 2\text{H}_2$), partial oxidation ($2\text{CH}_3\text{OH} + \text{O}_2 = 2\text{CO}_2 + 4\text{H}_2$), and especially methanol steam reforming (MSR, $\text{CH}_3\text{OH} + \text{H}_2\text{O} = \text{CO}_2 + 3\text{H}_2$) are considered as possible channels for hydrogen production.[1-4] Cu is a commercial catalyst for MSR[2]. However, it suffers from metal sintering at higher temperatures. Iwasa[5] et al discovered that the catalytic performance of Pd/ZnO to MSR is similar to that of Cu. Yet Pd/ZnO exhibits much higher thermal stability than Cu catalyst. [5, 6] Experimental [7-15] and theoretical [16-20] studies reveal that the nice catalytic performance of Pd/ZnO towards MSR reaction is owing to formation of PdZn alloys; 1:1 Pd-Zn alloy is one of the active components.

Recently Klötzer et al[21] investigated the catalytic properties of two PdZn model catalysts prepared by depositing 2 or 3 monolayers (MLs) of Zn onto Pd(111) and then annealing them at 500 and 650 K respectively for 10 minutes. The catalyst obtained at 500K (denoted as LT-alloy hereafter. In fact, samples prepared between 430 to 570 K exhibit the similar catalytic performance) shows ~100% CO_2 selectivity whereas poisonous CO is produced exclusively on the one prepared at 650K (HT-alloy). The low-energy ion scattering (LEIS) experiment indicates that the LT-alloy is a 1:1 multilayer PdZn surface alloy while the HT-alloy is interpreted to be a 1:1 monolayer PdZn alloy supported on Pd(111). According to Ref. 21 water dissociation can occur on the multilayer PdZn surface alloy. Dissociation product O or OH reacts with formaldehyde derived from methanol dehydrogenation, producing formic acid or other intermediate that finally converts to CO_2 . On the other hand, water keeps intact on the 1:1 monolayer surface alloy and formaldehyde has to undergo decomposition, leading to CO because there is no O or OH on the surface. Existence of hydroxyl group is verified on the LT-alloy,[21] supporting the above deduction.

However, our previous calculations on models based on the 1:1 ideal multilayer

PdZn(111) and 1:1 ideal monolayer PdZn film supported on Pd(111) show that the monolayer PdZn film supported on Pd(111) is more active for water dissociation than the multilayer PdZn(111), which is inconsistent with the above assumption adopted in Ref. 21. To rationalize the experimental phenomenon, we simulated the annealing process of two-monolayer Zn deposited Pd(111) surfaces using kinetic Monte Carlo (kMC) method, and identified the active center for water dissociation based on the kMC results. [22] We found the active center is a three-fold hollow site formed by three Zn atoms. We demonstrated that such hollow site is indeed active for water dissociation, and successfully rationalized the experimental phenomenon.

Methanol steam reforming begins with methanol dissociation. Previously we have carried out a systematic study of methanol dehydrogenation ($\text{CH}_3\text{OH} \rightarrow \text{CH}_3\text{O} \rightarrow \text{CH}_2\text{O} \rightarrow \text{CHO} \rightarrow \text{CO}$) on a series of Pd-Zn surface alloys using density functional theory (DFT).[23-26] Calculations were also performed on Pd(111) for comparison. The calculated binding energies of methanol, $\sim 0.3\text{eV}$, on the models used, are much lower than the dehydrogenation barrier, $\sim 1.0\text{eV}$. [27] These calculations indicate that methanol hardly dehydrogenates on PdZn alloy surfaces. This result implies that MSR cannot take place on PdZn alloys if it does start from methanol dehydrogenation, which contradicts the present viewpoint about the first step of MSR.

Considering the importance of methanol decomposition in understanding the MSR mechanism, in this chapter we use the active center model of PdZn alloy obtained from our kMC simulation to investigate methanol adsorption and dehydrogenation process. We show that methanol binds much more strongly on the three-fold hollow site formed by three Zn atoms, and methanol dehydrogenation to methoxy is possible. It is very likely the first step of MSR happens on sites formed by Zn atoms.

2 Model and computational details

Fig. 1 shows the unit cell structure active for water dissociation and will be used to study methanol dehydrogenation in this paper. The model is called kMC model. For

the details of KMC simulations, please refer to Ref.22. Supporting Information shows the simulated atomic arrangements for the top two layers.

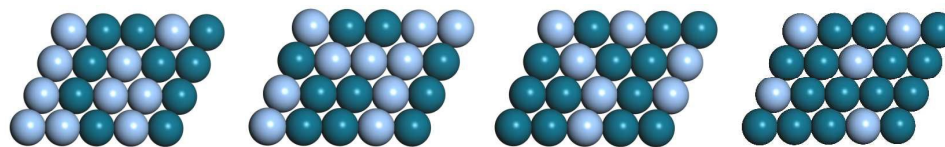


Figure 1 Illustration of surface unit cell structures of the kMC model derived from the kMC simulations. 1st layer, 2nd layer, 3rd and 4th layer (from left to right).

We adopted a vacuum spacing of 11 Å to separate periodic slabs. The bottom two layers was kept at the theoretical equilibrium bulk positions while the top two layers were fully relaxed during optimization. Optimizations were considered converged when the force on each ion smaller than 0.03 eV/Å. Periodic plane-wave density functional calculations combined with the climbing nudged elastic band (cNEB)[28, 29] were carried out to explore dehydrogenation reaction pathways of methanol on the surface. Ion-electron interactions were modeled within the framework of the projector augmented wave method[30, 31]. The generalized gradient approximation with the Perdew-Wang91 functional[32] was used to describe electron correlation. The geometries of all stationary points were located with the conjugate-gradient algorithm. A $2 \times 2 \times 1$ Monkhorst-Pack k-point mesh[33] was used to integrate over the Brillouin zone. All calculations were performed using the Vienna *ab initio* simulation package (VASP).[30, 34] Binding energies of an adsorbate, E_b , were calculated with $E_b = E_{\text{ads/sub}} - (E_{\text{sub}} + E_{\text{ads}})$. Here E_{sub} and E_{ads} are the total energies of the bare slab and the free adsorbate; $E_{\text{ads/sub}}$ is the total energy of the substrate with an adsorbate on it. With this definition, positive binding energies denote favorable adsorption processes.

3 Results and discussion

3.1 Adsorption of methanol, methoxy, formaldehyde and formyl

The binding energies, structural parameters of the most stable configurations for the species involved in methanol dehydrogenation are listed in Table 1. Also listed are the corresponding results calculated on regular PdZn(111) which is truncated from the

bulk structure and named as ideal model in this paper. In the following, we will briefly describe the most relevant features of these adsorption complexes.

Table 1 Binding energies (in eV), the most stable configuration and structural parameters (in angstrom) for intermediates involved in methanol dehydrogenation over Pd-Zn surface alloys. α defines the angle formed by the O-C bond axis and the surface normal.

<i>Species</i>		<i>Configuration</i>	E_b	d_{C-O}	d_{O-Zn}	$d_{O-Pd/C-Pd}^a$	α
CH ₃ OH	kMC model	η^1 -(O)	0.32	1.45	2.26	-	29
	Ideal model	η^1 -(O)	0.24	1.45	2.22	-	46
CH ₃ O	kMC model	η^3 -(O)	3.11	1.44	2.07-2.15	-	0
	Ideal model	η^3 -(O)	2.57	1.44	2.03	2.57	3
CH ₂ O	kMC model	η^2 -(C, O)	0.47	1.31	2.03	2.15	64
	Ideal model	η^2 -(C, O)	0.49	1.33	2.09	2.16	76
CHO	kMC model	η^1 -(C)	2.78	1.21	-	1.98	67
	Ideal model	η^2 -C- η^1 -O	2.38	1.28	2.07	2.12/2.13	74

Results for the ideal model are from Ref.[27]. ^a: $d_{O-Pd/C-Pd}$ refers to d_{O-Pd} for CH₃O and d_{C-Pd} for CH₂O.

a) Methanol CH₃OH

It is generally believed that methanol adsorbs via the lone pair of electrons of the oxygen to metallic surfaces, [35-37] which is also observed here. Binding energies reported previously on the ideal-model is 0.24 eV and the Zn-O distance is 2.22 Å.[27] We calculated a value of 0.32 eV on the kMC model, nearly 1.5 times as high as that on the ideal model. On the kMC model surface, methanol prefers the top site of Zn atom. The O-Zn distance, about 2.26 Å on the kMC model, almost as long as that on the ideal model. The C-O bond axis tilts away from the surface normal by 29° to let the lone pair of electrons of the oxygen atom better interact with the surface.

b) Methoxy CH₃O

Methoxy is an important intermediate during MSR process.[4, 8] On the ideal-model, CH₃O resides at a pseudo-hollow site, and the C-O axis tends to be

parallel to the surface normal with the corresponding value of α close to zero degree (Table 1). The binding energy is calculated to be 2.57 eV; the Zn-O distance is 2.03 Å.[27] On the kMC model CH₃O resides at the 3-fold hollow site formed by three Zn atoms. The C-O axis is normal to the surface. We obtained a binding energy of 3.11 eV on the kMC model, which is 0.54 eV higher than the result on the ideal model. The increase of binding energy is very likely due to one more O-Zn bond on the kMC model than on the ideal model because it is previously noted that species binding to surfaces via O atom prefer sites composing of more Zn atoms.[27] There are three O-Zn bonds on the kMC model, compared to two on the ideal model. The Zn-O distance ranges from 2.07 to 2.15 Å, compared to 2.03 Å on the ideal model.

c) Formaldehyde CH₂O

Formaldehyde is another important intermediate in methanol decomposition and synthesis,[5, 8] and formaldehyde adsorbs on transition metal surfaces in the η^2 -(C, O) mode the ideal model with the C atom bonding to a Pd and the O to a Zn atom. The Zn-O distance is 2.09 Å, and the binding energy is 0.49 eV.[27] We computed a binding energy of 0.47 eV on the kMC model; the Zn-O distance is 2.03 Å. On the kMC model formaldehyde also exists in the η^2 -(C, O) mode, as on the ideal model. The C-O bond length is 1.31 Å on the kMC model, compared with and 1.33 Å on the ideal model.

d) Formyl CHO

Previous theoretical study results in a binding energy of 2.38eV on the ideal model.[27] On the kMC model the binding energies are ~0.40 eV higher, 2.78 eV. Formyl on the ideal model belongs to the η^2 -C- η^1 -O configuration in which the C atom sits over a Pd-Pd bridge position and the O atom is on top of an adjacent Zn atom. [27] On the other hand, it is the η^1 -C configuration on the kMC model, where the C atom occupies a Pd top site.

3.2 Dehydrogenation mechanisms

In this subsection, we present dehydrogenation pathways of O-H bond breaking of methanol and subsequent C-H bond breaking of methoxy, formaldehyde and

formyl. Table 2 lists the reaction heats and energy barriers for each dehydrogenation step over the kMC model and ideal model surfaces. All the initial states (ISs), final states (FSs) and transition states (TSs) have been characterized to be either local minima or saddle points on potential energy surfaces (PES).

Table 2 Reaction Enthalpies (in kJ/mol) and energy barriers (in eV) of methanol dehydrogenation to CO over the ideal model and the kMC model.

Reaction	kMC model		Ideal_model	
	$\Delta H(\Delta H_0)$	$E_a(E_{a,0})$	$\Delta H(\Delta H_0)$	$E_a(E_{a,0})$
$\text{CH}_3\text{OH} \rightarrow \text{CH}_3\text{O} + \text{H}$	-55(-67)	0.55(0.39)	-25(-37)	0.91(0.69)
$\text{CH}_3\text{O} \rightarrow \text{CH}_2\text{O} + \text{H}$	90(75)	1.29(1.17)	60(45)	1.13(0.93)
$\text{CH}_2\text{O} \rightarrow \text{CHO} + \text{H}$	11(-2)	0.66(0.48)	-10(-24)	0.55(0.40)
$\text{CHO} \rightarrow \text{CO} + \text{H}$	-103(-113)	0.46(0.35)	-76(-87)	0.39(0.24)

*: Values in parentheses are ZPE corrected.

Methanol dehydrogenation can follow two pathways: the O-H bond breaking which produces methoxy ; and the C-H bond scission that yields hydroxymethyl. Schennach et al[38] concluded that the cleavage of methanolic C-H bond is preferred. Guo et al[39] demonstrated that the energy barrier of the C-H breaking is slightly lower than that of the O-H breaking. Experimentally both methoxy and hydroxymethyl were detected on Pd(111).[40-43] Static secondary ion mass spectrometry, X-ray photoelectron spectrometry and pulsed field desorption mass spectrometry measurements[44] show that the preferential pathway of methanol decomposition is $\text{CH}_3\text{OH} \rightarrow \text{CH}_3\text{O} \rightarrow \text{CH}_2\text{O} \rightarrow \text{CHO} \rightarrow \text{CO}$. In this work, we follow this proposed route. This choice is also based on the following considerations. Firstly, the experimental studies [44] support the O-H breaking as an initial step for methanol decomposition. Secondly methoxy is demonstrated to be an initial product of methanol dehydrogenation on Zn/Pd(111) surface in a very recent work. [8, 23, 25-27]

3.2.1 Dehydrogenation of methanol

The O-H bond breaking of CH₃OH starts from the approaching of the H atom to the surface. On the ideal model the O-H bond reaches 1.46 Å in the TS. The produced CH₃O group occupies the top site of the Zn atom through the O atom, and the atomic H stays at an adjacent Pd-Zn(Pd) bridge-like site. As reported before [16, 45] atop Zn and Pd-Zn(Pd) bridge sites are not most stable positions for CH₃O and H species respectively. They eventually move to a pseudo-fcc hollow site and a bridge-like position on the ideal model respectively. [27] On the kMC model (Figure 2), the O-H bond is 1.20 Å in the TS; the CH₃O group occupies the top site of the Zn atom; the H atom stays at the bridge site of the two Pd atoms. CH₃O finally moves to a 3-fold Zn hollow site and the H atom to the 3-fold Pd hollow site as shown in Figure 2. The O-H bond distance is 0.98 Å in the IS. It becomes 1.20 Å in the TS, compared with 1.46 Å on the ideal model.

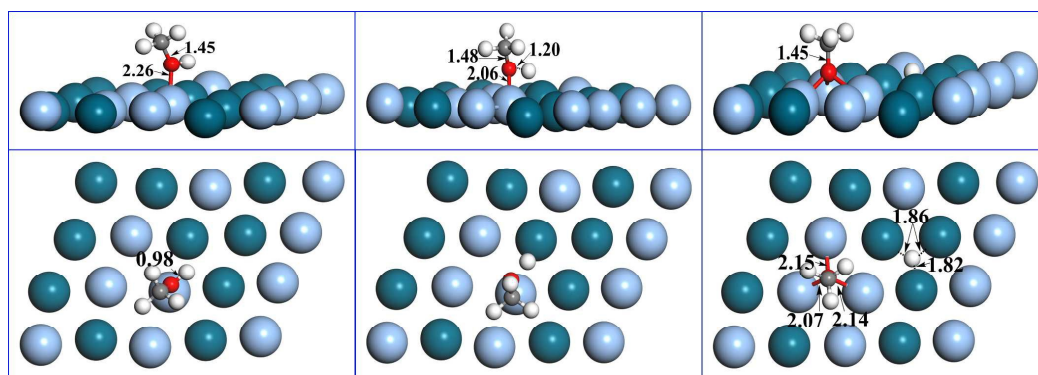


Figure 2 Dehydrogenation of methanol via O-H scission on PdZn alloy

The calculated barriers on the ideal model is 0.91 eV[27], and are much higher than 0.55 eV on the kMC model. Zero-point energy correction usually reduces the barrier by ~0.16 eV (Table 2). The calculated reaction energies, about 55 kJ/mol (exothermic) on the kMC model, are more than two times as high as that on the ideal model, which is only 25 kJ/mol.

3.2.2 Dehydrogenation of methoxy

As shown in Figure 3, CH₃O occupies a 3-fold hollow site formed by three Zn atoms. In the course of the reaction, the O atom moves from the hollow site to a Zn-Zn bridge position. Concomitantly, one of the methylic H gets closer to the surface

and interacts with a Pd atom. The C-H length increases from 1.10 Å in the IS to 1.34 Å in the TS. In the FS, CH₂O exhibits a di-sigma configuration (Figure 3). The H atom resides at a 3-fold Pd hollow site. This process is calculated to be endothermic by 90 kJ/mol. The corresponding energy barrier is 1.29 eV, compared with 1.13 eV on the ideal model, indicating that the 3-fold hollow site formed by three Zn atoms hinders the C-H bond scission of methoxy.

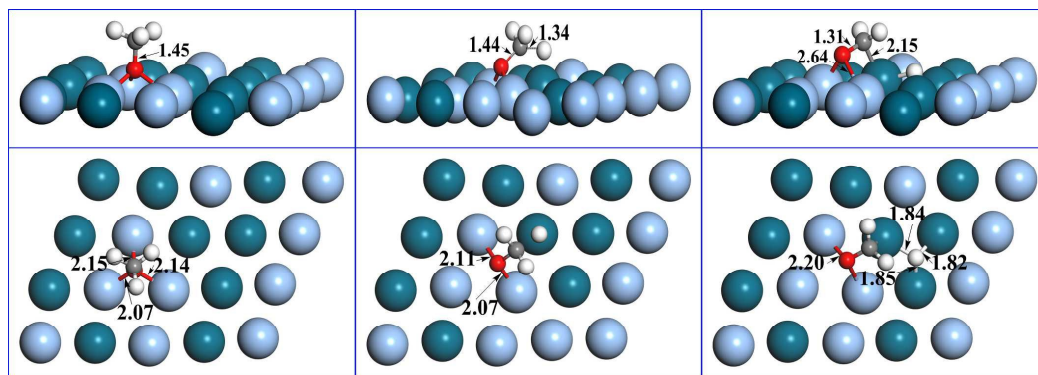


Figure 3 Dehydrogenation of methoxy to formaldehyde on the kMC model.

3.2.3 Dehydrogenation of formaldehyde

We chose the most stable η^2 -(C, O) configuration of formaldehyde as the IS for the dehydrogenation to formyl on our kMC model. The C-H length extends from 1.10 Å in the IS to 1.44 Å in the TS (Figure 4), compared with 1.62 Å on the ideal model. The C-O bond length shrinks from 1.31 Å in the IS to 1.24 Å in the TS. Meanwhile, the O-Zn and C-Pd bonds increase 0.27 Å and 0.63 Å, respectively. In the FS, the produced formyl is at a top Pd site, forming a η^1 -C configuration; The O-Zn bond is completely broken. The dissociated H atom moves to a nearby 3-fold hollow site formed by three Pd atoms, with two shorter H-Pd bonds of ~ 1.80 Å, and a longer H-Pd bond of 1.92 Å due to the bonding competition.

On the kMC model this step needs to overcome a barrier of 0.66 eV (Table 2) which is 0.11 eV higher than that on the ideal model. The calculated reaction energy is 11 kJ/mol whereas it is -10 kJ/mol on the ideal model. These results indicate that the sites formed by more Zn atoms are unfavorable for formaldehyde dehydrogenation both kinetically and thermodynamically.

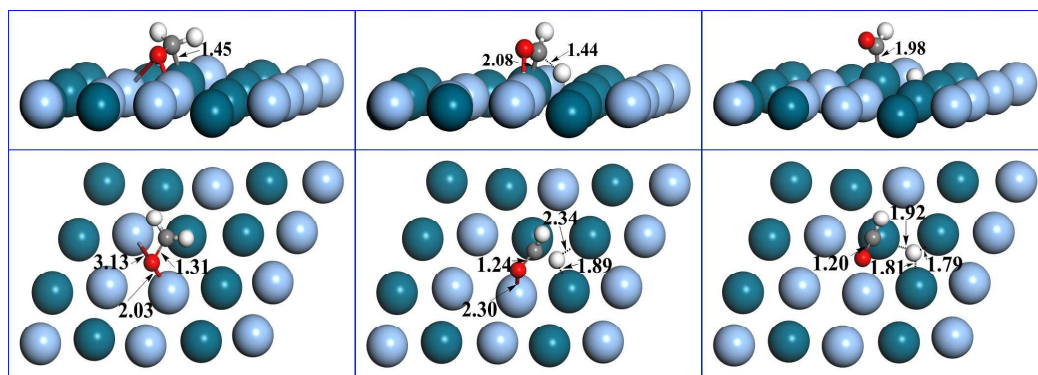


Figure 4 Dehydrogenation of formaldehyde on the LT-model.

3.2.4 Dehydrogenation of formyl

Figure 5 displays the dehydrogenation of formyl on the kMC model. In the IS, the formyl occupies the top site of a Pd atom with the C-Pd bond being 1.98 Å. In the TS, the CO fragment locates at the top Pd site with the C-O bond slightly tilted with respect to the surface and reduced from 1.21 Å in the IS to 1.18 Å in the TS. The C-H bond extends to 1.27 Å and the H atom occupies a top-like site. After the TS, the CO group moves to a 3-fold hollow site formed by three-Pd atoms, and the H atom to an adjacent Pd-Pd bridge site. As a comparison, we mention that on the ideal model, the CO group sits at a Pd-Pd bridge site, and the H atom occupies a 3-fold hollow site formed by one Zn and two Pd atoms in TS; in the FS, the CO group situates at a Pd-Pd bridge site and the H atom at an adjacent Pd-Pd bridge position.

Formyl dehydrogenation is an exothermic process as shown by the calculated reaction energy -103 kJ/mol that is slightly more exothermic than -76 kJ/mol on the ideal model. The calculated energy barrier is 0.46 eV, 0.07 eV higher than 0.39 eV on the ideal models. Both values are quite small, especially when ZPE correction is considered, indicating CO will be produced as soon as formyl is formed.

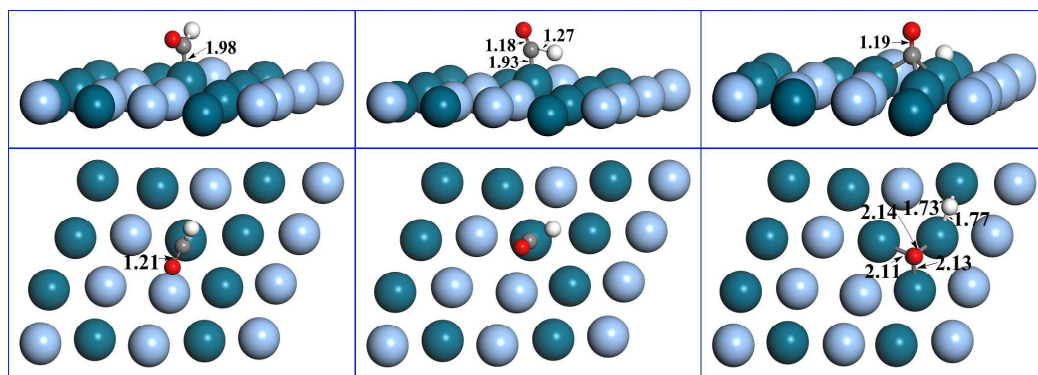


Figure 5 Dehydrogenation of formyl on the kMC model

3.3 Discussion

The calculated binding energies in Table 1 show that CH_3OH , CH_3O , CH_2O and CHO interact more strongly with the kMC model surface than with the ideal model surface. In particular, the binding energy of CH_3OH reaches 0.32 eV which is close to the ZPE corrected barrier (0.41 eV in Table 2) of methanol dehydrogenation. This situation remarkably contrasts with that on the ideal model where the binding energy of methanol is only 0.24 eV that is much lower than the ZPE corrected barrier of 0.69 eV. Obviously methanol is able to be converted into methoxy on the kMC model surface. Formation of methoxy is believed to be the first step of MSR, and previous studies on methanol dehydrogenation on ideal model always find this conversion difficult because of the low binding energy of methanol compared with the higher dehydrogenation barrier. Our present results imply that the first MSR step is very likely to take place at 3-fold hollow sites composing of Zn atoms.

The significant barrier reduction for methanol dehydrogenation to methoxy can be rationalized with the greatly increased binding energy of CH_3O , from 2.57 eV on the ideal model to 3.11 eV on the kMC model. The large increase of CH_3O binding energy can be understood with the previous conclusion that species interacts with the surface through oxygen atoms prefer sites with more Zn atoms[27]. As an evidence, we note that the adsorption site of CH_3O changes from an fcc site formed by two Zn and one Pd atom on the ideal model to an fcc position composed of three Zn atoms. The barrier of methoxy dehydrogenation to formaldehyde, 1.29 eV on the kMC model,

is 0.16 eV higher than that on the ideal surface. If the large binding energy of methoxy, >3.0 eV, is taken into consideration, one may infer that the active Zn-rich area will be blocked by the formed methoxy. In other words, although the Zn-rich site is active for methanol dehydrogenation, it will soon be blocked by the formed methoxy, and thus the subsequent steps will not take place. To find out whether this will happen or not in practice, we further examined methoxy dehydrogenation with co-adsorbed water. Existence of co-adsorbed water molecules on the surface is reasonable because as one of the reactants, water will definitely be populated on the surface. Our calculations show that with the co-adsorbed water the barrier of methoxy dehydrogenation reduces from 1.29 eV to 0.87 eV which is 0.26 eV lower than that on the ideal surface (see Table S1). This result demonstrates that the Zn-rich area will not be blocked by methoxy and the subsequent dehydrogenation can be continued. This result also indicates the importance of water in refreshing the Zn-rich site. It is worthy to mention that recently Huang and his co-workers reported a barrier of 1.16 eV without ZPE correction included for methoxy dehydrogenation to formaldehyde on the ideal surface in the presence of co-adsorbed water[46], and previously we found that OH group does not facilitate methoxy dehydrogenation[47]. The binding energies of CH₂O, from 0.49 eV on the ideal model to 0.47 eV on the kMC model, are close to each other. For CHO, its adsorption configuration changes from η^2 -C- η^1 -O on the ideal model to η^1 -C mode on the kMC model. With the configuration change, the binding energy increases by 0.40 eV, from 2.38 eV on the ideal model to 2.78 eV on the kMC model.

The above results show, species whether it binds to the surface using O or C, becomes more stable on the kMC model. The total Pd:Zn ratio of the kMC model is very close to 1:1 for the ideal model. The main difference is that the atomic arrangement in kMC model is less homogeneous than that of the ideal model. Existence of such inhomogeneity can be expected either due to the finite time of catalyst preparation that cannot guarantee all the atoms to be in their equilibrium position, or due to adsorption segregation (species like CH₃O that interacts with the surface using O atom would create ensembles formed by Zn atoms). Likely both play

the role. No matter what the reason is, inhomogeneous Pd-Zn alloy structures exhibit quite differently to MSR. Apparently one should extend studies of MSR using models beyond those (like the ideal model) adopted from regular bulk structure.

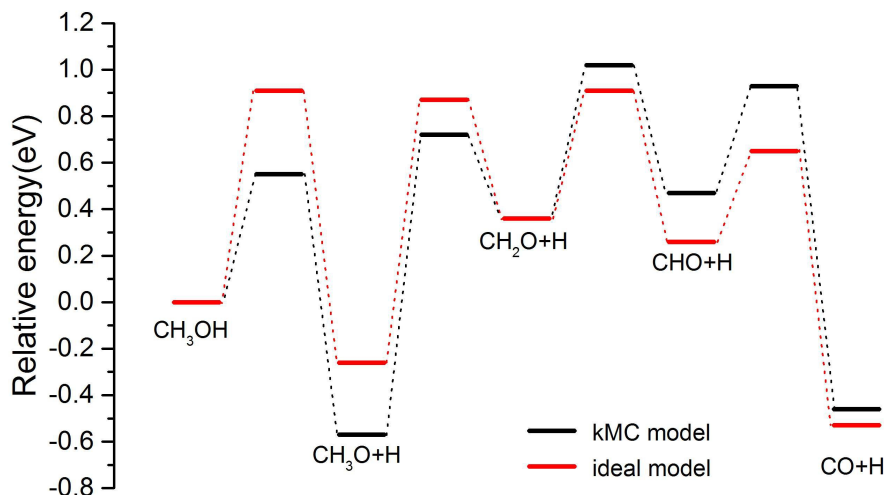


Figure 6 Comparison of potential energy surfaces of methanol dehydrogenation to CO on the kMC model (black) and the ideal model (red) surfaces.

Figure 6 shows the overall potential energy surface (PES) of methanol dehydrogenation to CO on the kMC model (black line) and the ideal model (red line) surfaces. The calculated PES clearly shows that the O-H bond cleavage of CH₃OH is greatly enhanced on the kMC model. On the other hand, the C-H bond breaking of CH₃O, CH₂O and CHO becomes harder.

The calculation PES sheds some light on the MSR mechanism catalyzed by Pd/ZnO. According to the PES, dehydrogenation of CHO to CO is quite easy. Since experimentally only a trace amount of CO is yielded in the course of MSR on the PdZn model catalyst prepared at low temperature (430~570K)[21], this experimental fact may be due to: (i) CHO cannot be formed largely from CH₂O owing to a much more faster reaction than CH₂O→CHO+H. A possible reaction is combination of CH₂O with species such as surface O or hydroxyl groups, resulting in formate which ultimately decomposes to CO₂ and H₂. (ii) The produced CHO undergoes a reaction that is much facile than CHO→CO+H, to become another species that serves as precursors for CO₂ formation. This possibility is less likely because dehydrogenation

of CHO only needs to overcome a barrier of 0.3 eV. (iii) $\text{CHO} \rightarrow \text{CO} + \text{H}$ takes place, but formed CO transforms into CO_2 . This route is experimentally excluded. Therefore among the three possibilities, the first one is most likely. According to our PES, dehydrogenation of CH_2O to CHO is more difficult on the kMC model than on the ideal model. This implies that sites with more Zn atoms would inhibit the conversion of CH_2O to CHO, and thus help improve the selectivity to CO_2 .

Recently, Loffreda et al[48] found that there is a nice correlation between the total energies of ISs and the total energies of TSs. Figure 7(a) shows the classical BEP relationship reflecting the energy barrier of the three C-H bond scission steps as a function of the corresponding reaction heat. The linear correlation coefficient is 0.70. Figure 7(b) correlates the energy of transition states (E^{TS}) of C-H bond scission and the energy of the corresponding initial states (E^{IS}). A correlation coefficient of 1.0 is obtained, indicating the newly proposed relationship is better than the classical one, and may be extended to other cases.

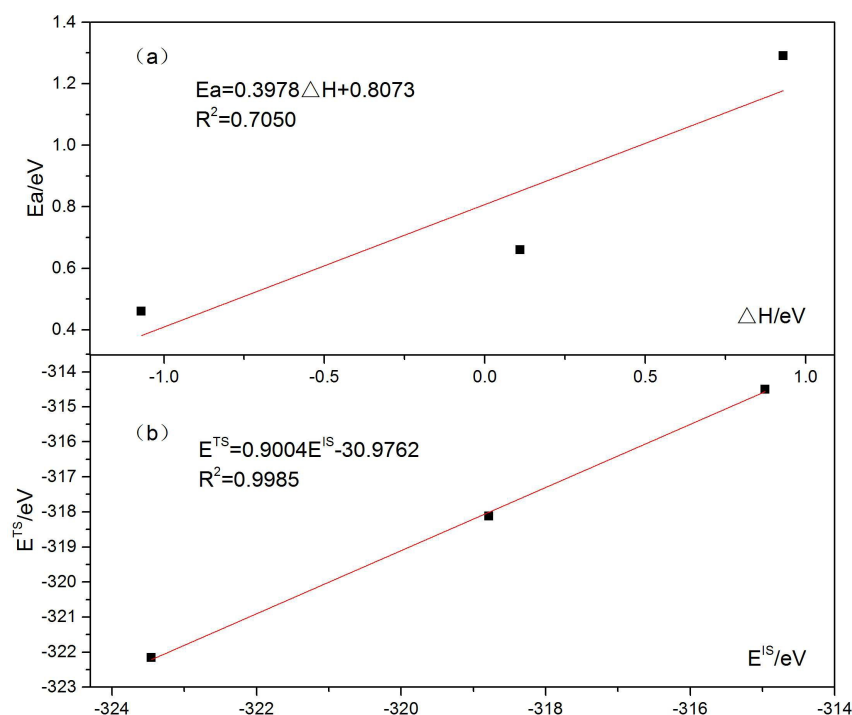


Figure 7 Relationship between the energy barriers of the three C-H bond scission and the reaction energies (a) and between the energy of initial states and transition states (b) on LT-alloy.

4 Conclusions

Methanol dehydrogenation to CO on the kMC models has been explored using periodic DFT calculations. Our calculations show that CH₃OH and CH₂O bind weakly to the alloy surface than CH₃O and CHO. Compared with the situation on the ideal model surface, all the studied species bond more strongly to the kMC model than to the ideal alloy surface. We show that sites with more Zn atoms favor methanol dehydrogenation to methoxy and formation of methoxy is possible. On the other hand, the C-H bond breaking of CH₃O, CH₂O and CHO becomes more difficult. The present study solves the problem that the binding energy of methanol on PdZn alloy surface is too small to enable the occurrence of methanol dehydrogenation to methoxy, the starting step of MSR. It also reveals that active sites with more Zn content favor methanol dehydrogenation, but hinders the formation of CO, and thus are favorable for the selectivity of CO₂. Finally we show that water is important for reviving the active sites.

Taking studies on both water dissociation reported in Ref. [22] and methanol dehydrogenation in this paper, one can conclude that whether MSR starts from methanol dehydrogenation or water dissociation, it is very likely that the first step, O-H bond breaking, takes place on the 3-fold hollow sites formed by three Zn atoms.

Acknowledgements

The authors acknowledge the financial support from the national key basic research development program of China (973 Program) 2011CB808604 and the Natural Science Foundation of China No.21273103 and 20973090. All calculations were done in the high performance calculation center of Nanjing University.

References

- [1] L. Alejo, R. Lago, M.A. Pena, J.L.G. Fierro, Partial oxidation of methanol to produce hydrogen over Cu-Zn-based catalysts, *Applied Catalysis a-General*, 162 (1997) 281-297.
- [2] B.A. Peppley, J.C. Amphlett, L.M. Kearns, R.F. Mann, Methanol-steam reforming

- on Cu/ZnO/Al₂O₃. Part 1: The reaction network, *Appl. Catal. A-Gen.*, 179 (1999) 21-29.
- [3] S.T. Liu, K. Takahashi, K. Uematsu, M. Ayabe, Hydrogen production by oxidative methanol reforming on Pd/ZnO catalyst: effects of the addition of a third metal component, *Applied Catalysis a-General*, 277 (2004) 265-270.
- [4] T.V. Choudhary, D.W. Goodman, CO-free fuel processing for fuel cell applications, *Catalysis Today*, 77 (2002) 65-78.
- [5] N. Iwasa, N. Takezawa, New supported Pd and Pt alloy catalysts for steam reforming and dehydrogenation of methanol, *Topics in Catalysis*, 22 (2003) 215-224.
- [6] N. Takezawa, N. Iwasa, Steam reforming and dehydrogenation of methanol: Difference in the catalytic functions of copper and group VIII metals, *Catalysis Today*, 36 (1997) 45-56.
- [7] A. Karim, T. Conant, A. Datye, The role of PdZn alloy formation and particle size on the selectivity for steam reforming of methanol, *Journal of Catalysis*, 243 (2006) 420-427.
- [8] E. Jerero, J.M. Vohs, Zn modification of the reactivity of Pd(111) toward methanol and formaldehyde, *Journal of the American Chemical Society*, 130 (2008) 10199-10207.
- [9] A.M. Karim, T. Conant, A.K. Datye, Controlling ZnO morphology for improved methanol steam reforming reactivity, *Physical Chemistry Chemical Physics*, 10 (2008) 5584-5590.
- [10] A. Tamtoegl, M. Kratzer, J. Killman, A. Winkler, Adsorption/desorption of H₂ and CO on Zn-modified Pd(111), *Journal of Chemical Physics*, 129 (2008).
- [11] E. Jerero, J.M. Vohs, Exploring the role of Zn in PdZn reforming catalysts: adsorption and reaction of ethanol and acetaldehyde on two-dimensional PdZn alloys, *Journal of Physical Chemistry C*, 113 (2009) 1486-1494.
- [12] E. Jerero, J.M. Vohs, Reaction of formic acid on Zn-modified Pd(111), *Catalysis Letters*, 130 (2009) 271-277.
- [13] M. Kratzer, A. Tamtoegl, J. Killmann, R. Schennach, A. Winkler, Preparation and calibration of ultrathin Zn layers on Pd(111), *Applied Surface Science*, 255 (2009) 5755-5759.
- [14] W. Stadlmayr, S. Penner, B. Klötzer, N. Memmel, Growth, Thermal stability and structure of ultrathin Zn-layers on Pd(111), *Surface Science*, 603 (2009) 251-255.
- [15] G. Weirum, M. Kratzer, H.P. Koch, A. Tamtoegl, J. Killmann, I. Bako, A. Winkler, S. Surnev, F.P. Netzer, R. Schennach, Growth and desorption kinetics of ultrathin Zn layers on Pd(111), *Journal of Physical Chemistry C*, 113 (2009) 9788-9796.
- [16] Z.X. Chen, K.M. Neyman, K.H. Lim, N. Rosch, CH₃O decomposition on PdZn(111), Pd(111), and Cu(111). A theoretical study, *Langmuir*, 20 (2004) 8068-8077.
- [17] Z.X. Chen, K.M. Neyman, A.B. Gordienko, N. Rosch, Surface structure and stability of PdZn and PtZn alloys: Density-functional slab model studies, *Physical Review B*, 68 (2003).
- [18] Z.X. Chen, K.M. Neyman, N. Rösch, Theoretical study of segregation of Zn and Pd in Pd-Zn alloys, *Surface Science*, 548 (2004) 291-300.

- [19] K.M. Neyman, K.H. Lim, Z.-X. Chen, L.V. Moskaleva, A. Bayer, A. Reindl, D. Borgmann, R. Denecke, H.-P. Steinrueck, N. Rösch, Microscopic models of PdZn alloy catalysts: structure and reactivity in methanol decomposition, *Physical Chemistry Chemical Physics*, 9 (2007) 3470-3482.
- [20] H.P. Koch, I. Bako, R. Schennach, Adsorption of small molecules on a (2 x 1) PdZn surface alloy on Pd(111), *Surface Science*, 604 (2010) 596-608.
- [21] C. Rameshan, W. Stadlmayr, C. Weilach, S. Penner, H. Lorenz, M. Haevecker, R. Blume, T. Rocha, D. Teschner, A. Knop-Gericke, R. Schlögl, N. Memmel, D. Zemlyanov, G. Rupprechter, B. Klötzer, Subsurface-controlled CO₂ selectivity of PdZn near-surface alloys in H₂ generation by methanol steam reforming, *Angewandte Chemie-International Edition*, 49 (2010) 3224-3227.
- [22] Z.-X. Chen Feng Cheng, Kinetic Monte Carlo simulation of PdZn alloying and density functional study of PdZn surface reactivity towards water dissociation, *ChemCatChem communication*, (2015).
- [23] Y. Huang, Z.-X. Chen, First-principles study of water dissociation on PdZn near surface alloys, *Journal of Physical Chemistry C*, 115 (2011) 18752-18760.
- [24] Y. Huang, W. Ding, Z.-X. Chen, Effect of Zn on the adsorption of CO on Pd(111), *Journal of Chemical Physics*, 133 (2010).
- [25] Y. Huang, X. He, Z.-X. Chen, First-principles study towards the reactivity of the Pd(111) surface with low Zn deposition, *Journal of Chemical Physics*, 134 (2011).
- [26] Y. Huang, X. He, Z.-X. Chen, Density functional study of methanol decomposition on clean and O or OH adsorbed PdZn(111), *Journal of Chemical Physics*, 138 (2013).
- [27] Y. Huang, Z.-X. Chen, Density functional investigations of methanol dehydrogenation on Pd-Zn surface alloy, *Langmuir*, 26 (2010) 10796-10802.
- [28] G. Henkelman, H. Jonsson, Improved tangent estimate in the nudged elastic band method for finding minimum energy paths and saddle points, *Journal of Chemical Physics*, 113 (2000) 9978-9985.
- [29] G. Henkelman, B.P. Uberuaga, H. Jonsson, A climbing image nudged elastic band method for finding saddle points and minimum energy paths, *Journal of Chemical Physics*, 113 (2000) 9901-9904.
- [30] P.E. Blochl, Projector augmented-wave method, *Phys. Rev. B*, 50 (1994) 17953-17979.
- [31] G. Kresse, J. Furthmuller, Efficiency of ab-initio total energy calculations for metals and semiconductors using a plane-wave basis set, *Computational Materials Science*, 6 (1996) 15-50.
- [32] J.P. Perdew, Y. Wang, Accurate and simple analytic representation of the electron-gas correlation-energy, *Phys. Rev. B*, 45 (1992) 13244-13249.
- [33] H.J. Monkhorst, J.D. Pack, Special points for brillouin-zone integrations, *Phys. Rev. B*, 13 (1976) 5188-5192.
- [34] G. Kresse, J. Hafner, Ab-Initio molecular-dynamics simulation of the liquid-metal amorphous-semiconductor transition in germanium, *Phys. Rev. B*, 49 (1994) 14251-14269.
- [35] M. Mavrikakis, M.A. Barteau, Oxygenate reaction pathways on transition metal

- surfaces, *Journal of Molecular Catalysis a-Chemical*, 131 (1998) 135-147.
- [36] M. Bowker, R.J. Madix, XPS, UPS and thermal-desorption studies of alcohol adsorption on Cu(110) .1. Methanol, *Surface Science*, 95 (1980) 190-206.
- [37] B.A. Sexton, A.E. Hughes, A Comparison of weak molecular adsorption of organic-molecules on clean copper and platinum surfaces, *Surface Science*, 140 (1984) 227-248.
- [38] R. Schennach, A. Eichler, K.D. Rendulic, Adsorption and desorption of methanol on Pd (111) and on a Pd/V surface alloy, *Journal of Physical Chemistry B*, 107 (2003) 2552-2558.
- [39] R. Jiang, W. Guo, M. Li, D. Fu, H. Shan, Density functional investigation of methanol dehydrogenation on Pd(111), *Journal of Physical Chemistry C*, 113 (2009) 4188-4197.
- [40] J.A. Gates, L.L. Kesmodel, Methanol adsorption and decomposition on clean and oxygen precovered palladium (111), *Journal of Catalysis*, 83 (1983) 437-445.
- [41] R.J. Levis, Z.C. Jiang, N. Winograd, Thermal-decomposition of CH₃OH adsorbed on Pd(111) - a new reaction pathway involving CH₃ formation, *Journal of the American Chemical Society*, 111 (1989) 4605-4612.
- [42] H. Yang, J.L. Whitten, Adsorption of formyl on Ni(100), *Langmuir*, 11 (1995) 853-859.
- [43] J.J. Chen, Z.C. Jiang, Y. Zhou, B.R. Chakraborty, N. Winograd, Spectroscopic studies of methanol decomposition on Pd(111), *Surface Science*, 328 (1995) 248-262.
- [44] N. Kruse, M. Rebholz, V. Matolin, G.K. Chuah, J.H. Block, Methanol decomposition on Pd(111) Single-Crystal Surfaces, *Surface Science*, 238 (1990) 457-462.
- [45] K.H. Lim, Z.-X. Chen, K.M. Neyman, N. Rösch, Comparative theoretical study of formaldehyde decomposition on PdZn, Cu, and Pd surfaces, *Journal of Physical Chemistry B*, 110 (2006) 14890-14897.
- [46] Z.Q. Huang, B. Long, C.R. Chang, A theoretical study on the catalytic role of water in methanol steam reforming on PdZn(111), *Catal. Sci. Technol.*, 5 (2015) 2935-2944.
- [47] Y. Huang, Theoretical study of methanol steam reforming catalyzed by pdzn alloy, *Doctoral Dissertation 2011*, NanJing University, China.
- [48] D. Loffreda, F. Delbecq, F. Vigne, P. Sautet, Fast prediction of selectivity in heterogeneous catalysis from extended bronsted-evans-polanyi relations: a theoretical insight, *Angewandte Chemie-International Edition*, 48 (2009) 8978-8980.